https://doi.org/10.5194/hess-2019-254
Preprint. Discussion started: 28 May 2019

Hydrology and Earth System Sciences
Open Access
Discussions

Temporal-dependent effects of rainfall characteristics on inter-/intra-event stemflow variability in two xerophytic shrubs

Chuan Yuan[1, 2, 3], Guangyao Gao[2], Bojie Fu[2], Daming He[1, 3], Xingwu Duan[1, 3], and Xiaohua Wei[4]

[1]Institute of International Rivers and Eco–security, Yunnan University, Kunming 650091, China
[2]State Key Laboratory of Urban and Regional Ecology, Research Center for Eco-Environmental Sciences, Chinese Academy of Sciences, Beijing 100085, China
[3]Yunnan Key Laboratory of International Rivers and Trans-boundary Eco–security, Kunming 650091, China
[4]Department of Earth, Environmental and Geographic Sciences, University of British Columbia (Okanagan campus), Kelowna, British Columbia, V1V 1V7, Canada

Correspondence: Guangyao Gao (gygao@rcees.ac.cn)

Abstract

Stemflow is important for recharging root-zone soil moisture in arid regions. Previous studies have generally focused on stemflow volume, efficiency and influential factors but have failed to depict temporal stemflow processes and quantify their relationships with rainfall characteristics within events, particularly for xerophytic shrubs. Here, we measured the stemflow volume, intensity, duration and time lags to rain events of two xerophytic shrub species (*Caragana korshinskii* and *Salix psammophila*) and rainfall characteristics

https://doi.org/10.5194/hess-2019-254
Preprint. Discussion started: 28 May 2019

for 54 events in the Liudaogou catchment of the Loess Plateau, China, during the 2014-2015 rainy seasons. The results indicated that stemflow dynamics were well synchronized to rainfall processes. The stemflows of *C. korshinskii* and *S. psammophila* had larger average intensities (4.7±1.5 and 4.8±1.6 mm·h^{-1}, respectively) than that of rain at the event scale (4.5±1.0 mm·h^{-1}), and the stemflows were even more intense (20.3±10.4 and 16.9±8.8 mm·h^{-1}, respectively) than that of rain at 10-min intervals (10.9±2.1 mm·h^{-1}). The average stemflow durations of *C. korshinskii* and *S. psammophila* (3.8±0.8 and 3.4±0.9 h, respectively) were shorter than the rainfall duration (4.7±0.8 h). Tested by a multiple correspondence analysis and stepwise regression, rainfall amount and duration controlled stemflow volume and duration, respectively, at the event scale by linear relationships (p<0.01). Rainfall intensity and raindrop momentum controlled stemflow intensity and time lags for both species at the intra-event scale by linear or power relationships (p<0.01). Rainfall intensity was the key factor for the stemflow process of *C. korshinskii*, whereas raindrop momentum had the greatest influence on the stemflow process of *S. psammophila*. Rainfall characteristics had temporal-dependent influences on corresponding stemflow variables, and the influence also depended on specific species.

1 Introduction

Stemflow directs intercepted rains from the canopy to the trunk base. The funnel-shaped canopy and underground preferential paths, i.e., roots, worm paths and soil macropores, converge rains to recharge the root-zone moisture (Johnson and Lehmann, 2006; Li et al., 2008). Stemflow is important to concentrate water (Levia and Germer,

https://doi.org/10.5194/hess-2019-254
Preprint. Discussion started: 28 May 2019

Hydrology and Earth System Sciences
Open Access
Discussions

2015), nutrients (Dawoe et al., 2018), pathogens (Garbelotto et al., 2003) and bacteria (Bittar et al., 2018) from the phyllosphere into the pedosphere (Teachey et al., 2018), even though stemflow accounts for only a minimal part of rainfall amount (RA) (6.2%) in contrast to throughfall (69.8%) and interception loss (24.0%) in water-stressed regions (Magliano et al., 2019). Stemflow greatly contributes to the survival of xerophytic plant species (Návar, 2011), the maintenance of patch structures in arid areas (Kéfi et al., 2007), and the normal functioning of rainfed dryland ecosystems (Wang et al., 2011).

To quantify the ecohydrological importance of stemflow, numerous studies have been conducted on stemflow production and efficiency from various aspects, including stemflow volume (mL), depth (mm), percentage (%), funnelling ratio (unitless), and productivity ($mL \cdot g^{-1}$) (Herwitz, 1986; Yuan et al., 2016; Zabret et al., 2018; Yang et al., 2019). By applying automatic recording devices, the stemflow process has been gradually determined at 1-h intervals (Spencer and van Meerveld, 2016), 5-min intervals (André et al., 2008; Levia et al., 2010) and 2-min intervals (Dunkerley, 2014). This determination allowed the calculation of stemflow intensity ($mm \cdot h^{-1}$) (Germer et al., 2010), speed ($mL \cdot min^{-1}$) (Yang, 2010) and time lag after rain (Cayuela et al., 2018). Differing from an event-based calculation, the stemflow process provided insights into the fluctuation of stemflow production at a high temporal resolution. This process permits a better interpretation of the "hot moment" and "hot spot" effects of many ecohydrological processes (Bundt et al., 2001; McClain et al., 2003). Quantifying short-intensity burst and temporal characteristics of stemflow shed light on the dynamic process and pulse nature of stemflow (Dunkerley, 2019).

Stemflow cannot be initialled after canopies were saturated by the rains (Martinez-Meza and Whitford, 1996). The minimal RA needed to start stemflow is usually calculated by regressing stemflow volume with RA for different plant species or canopy states (Levia and Germer, 2015). In the leaf period, stemflow starts when rains are greater than 10.9 mm and 2.5-3.4 mm for oak and beech tress, respectively, in Belgium, and in the leafless period, the minimal RA for stemflow generation is 6.0 mm and 1.5-1.9 mm for these two species (André et al., 2008; Staelens et al., 2008). In comparison, a lower amount of rain,0.4-2.2 mm, can generally initiate stemflow of xerophytic shrubs (Yuan et al., 2017). Stemflow also frequently continues after rains due to the rainwater retained on the canopy surface (Iida et al., 2017). *Salix psammophila* and an open tropical forest start stemflow 5-10 min and 15 min later than the beginning of a rain event in the Mu Us desert of China (Yang, 2010) and the Amazon basin of Brazil (Germer et al., 2010), respectively. However, 1 h and 1.5 h are needed to start stemflow after the beginning of a rain event for pine and oak trees in north-eastern Spain, respectively (Cayuela et al., 2018). For *S. psammophila*, stemflow is maximized 20-210 min after the beginning of a rain event (Yang, 2010), and stemflow ceased 11 h after rain stopped in an open tropical forest (Germer et al., 2010). Stemflow time lags are critical indicators for depicting the stemflow process and are important for developing process-based hydrological models. However, stemflow time lags have not been systematically studied for xerophytic shrubs.

The preferential paths at the underside of branches for delivering stemflow complicates stemflow processes within events (Dunkerley, 2014). The influences of bark microrelief on stemflow are strongly affected by dynamic rain processes, such as rainfall intensity and raindrop striking within events (Van Stan and Levia, 2010). While exceeding the holding capacity of branches, high rainfall intensity can overload and interrupt this preferential path (Carlyle-Mose and Price, 2006). Raindrops hit the canopy surface and create splashes on the surface. This process is conducive to wetting branches at the lower layers and accelerating the establishment of the preferential paths of stemflow transportation (Bassette and Bussière, 2008). Nevertheless, the interaction between the stemflow process and intra-event rainfall characteristics has not been substantially studied.

This study was designed at the event and process scales to investigate inter-/intra-event stemflow variability of two xerophytic shrubs. Stemflow volume, intensity and temporal dynamics of *Caragana korshinskii* and *S. psammophila* were recorded during 54 rainfall events in the 2014–2015 rainy seasons on the Loess Plateau of China. Temporal dynamics were expressed as stemflow duration and time lags of stemflow generation, maximization and cessation to the start of rain events. Raindrop momentum was introduced to represent the comprehensive effects of raindrop size, velocity, inclination angle and kinetic energy on the stemflow process. This study specifically aimed to (1) depict the stemflow process in terms of stemflow intensity and temporal dynamics, (2) identify the dominant rainfall characteristics influencing inter-/intra-event stemflow variables, and (3) quantify the relationships between stemflow process variables and rainfall characteristics. Achieving these objectives would advance our knowledge of process-based stemflow production to better understand the pulse nature of stemflow and its interactions with dynamic rain processes.

2 Materials and Methods

https://doi.org/10.5194/hess-2019-254
Preprint. Discussion started: 28 May 2019

2.1 Site description

This study was conducted in the Liudaogou catchment (110°21′–110°23′E, 38°46′–38°51′N) in Shenmu city, Shaanxi Province, China, during the 2014–2015 rainy seasons. This catchment is 6.9 km^2 and 1094–1273 m above sea level (m.a.s.l.). A semiarid continental climate prevails in this area. The mean annual precipitation (MAP) is 414 mm (1971–2013). Most MAP (77%) occurs from July to September (Jia et al., 2013). The mean annual potential evaporation is 1337 mm (Yang et al., 2019). The mean annual temperature is 9.0 °C. The dominant shrubs include *C. korshinskii*, *S. psammophila*, and *Amorpha fruticosa*. The dominant grasses are *Artemisia capillaris*, *Artemisia sacrorum*, *Medicago sativa*, *Stipa bungeana*, etc.

C. korshinskii and *S. psammophila* are two representative xerophytic shrub species. They have inverted-cone crowns and no trunks, with multiple branches running obliquely from the base. As modular organisms and multi-stemmed shrub species, their branches live as independent individuals and compete with each other for water and light (Firn, 2004). Two plots were established in the southwestern catchment for these two xerophytic shrubs planted in the 1990s (Fig. 1). *C. korshinskii* and *S. psammophila* plots share similar stand conditions with elevations of 1179 and 1207 m.a.s.l., slopes of 13° and 18°, and sizes of 3294 and 4056 m^2, respectively. The *C. korshinskii* plot has a ground surface of loess and aspect of 224°, while the *S. psammophila* plot has a ground surface of sand and an aspect of 113°.

2.2 Meteorological measurements and calculations

A meteorological station was installed at the experimental plot of *S. psammophila* to

https://doi.org/10.5194/hess-2019-254
Preprint. Discussion started: 28 May 2019

record rainfall characteristics and wind speed (WS, $m \cdot s^{-1}$). The Onset® (Onset Computer Corp., USA) RG3-M tipping-bucket rain gauges (with a diameter of 15.24 cm and a resolution of 0.2 mm) recorded the rain amount and timing of incident rains. Discrete rainfall events were defined by a measurable RA of 0.2 mm (the resolution limit of the RG3-M rain gauge) and the smallest 4-h gap without rains (the analogue period of time to dry canopies from antecedent rains) (Giacomin and Trucchi, 1992; Zhang et al., 2015; Yang et al., 2019). WS was recorded by wind sensors (Model 03002, R. M. Young Company, USA) and logged at 10-min intervals by a datalogger (Model CR1000, Campbell Scientific Inc., USA). For the 0.8-km distance between the two plots, the meteorological data were also applied to the *C. korshinskii* plot.

Rainfall characteristics were calculated, including the RA (mm), rainfall duration (RD, h), rainfall interval (RI, h), the average and 10-min maximum rainfall intensity of incident rains (I and I_{10}, respectively, $mm \cdot h^{-1}$), and the 10-min average rainfall intensity after rain begins (I_{b10}, $mm \cdot h^{-1}$) and before rain ends (I_{e10}, $mm \cdot h^{-1}$). Raindrop traits include diameter (D, mm) (Herwitz and Slye, 1995), terminal velocity (V, $m \cdot s^{-1}$) (Carlyle-Moses and Schooling, 2015), and average inclination angle (θ, °) (Herwitz and Slye, 1995; Van Stan et al., 2011). By assuming a perfect sphere of a raindrop (Uijlenhoet and Torres, 2006), the average raindrop momentum in the vertical direction (F, $mg \cdot m \cdot s^{-1}$) was computed to comprehensively represent the raindrop morphology and energy (Brandt, 1990; Kimble, 1996).

$$D = 2.23 \times (0.03937 \times I)^{0.102} \quad (1)$$

$$V = 3.378 \times \ln(D) + 4.213 \quad (2)$$

https://doi.org/10.5194/hess-2019-254
Preprint. Discussion started: 28 May 2019

$$\tan \theta = WS / V \quad (3)$$

$$F_0 = M \times V = (1/6 \times \rho \times \pi \times D^3) \times V \quad (4)$$

$$F = F_0 \times \cos \theta \quad (5)$$

where I is the average rainfall intensity of incident rains ($mm \cdot h^{-1}$), M is the average raindrop mass (g), and F_0 is the average raindrop momentum ($mg \cdot m \cdot s^{-1}$). ρ is the density of freshwater at standard atmospheric pressure and 20℃ (0.998 $g \cdot cm^{-3}$). WS is the average wind speed of incident rains ($m \cdot s^{-1}$). The 10-min maximum raindrop momentum (F_{10}, $mg \cdot m \cdot s^{-1}$) and the average raindrop momentum at the first and last 10 min (F_{b10} and F_{e10}, respectively, $mg \cdot m \cdot s^{-1}$) could also be calculated with I_{10}, I_{b10} and I_{e10} during incident rains, respectively.

2.3 Experimental branch selection and measurements

This study focused on the branch stemflow of *C. korshinskii* and *S. psammophila*. By selecting four 20-year-old shrubs of each species with similar crown areas and heights (5.1±0.3 m^2 and 2.1±0.2 m for *C. korshinskii* and 21.4±5.2 m^2 and 3.5±0.2 m for *S. psammophila*, respectively), the variance in canopy traits was neglected. The isolated canopies guaranteed that they were exposed to similar rainfall characteristics. We measured branch morphologies of all 180 and 261 branches of experimental shrubs of *C. korshinskii* and *S. psammophila*, respectively. Branch basal diameter (BD) was measured with a Vernier calliper (Model 7D-01150, Forgestar Inc., Germany). Branch length (BL) and branch angle (BA) were estimated with a measuring tape and pocket geologic compass (Model DQL-8, Harbin Optical Instrument Factory, China), respectively. Then, the branches were grouped into five BD categories of 5–10 mm, 10–15 mm, 15–18 mm, 18–25 mm and >25 mm. Two branches with median BDs were selected in each category for stemflow recording. These branches had no intercrossing with neighbouring branches and no turning point in height from branch tip to base. The canopy-skirt locations avoided over-shading by the upper layer branches and permitted convenient measurements. Since there were not sufficient >25-mm branches for the *C. korshinskii* shrubs and the tipping-bucket rain gauges malfunctioned at the 18–25-mm branches of *S. psammophila*, stemflow data were not available in these BD categories. In total, stemflow was automatically recorded at 7 branches for each species (Table 1).

2.4 Stemflow measurements and calculations

We applied aluminium foil collars to trap stemflow. They were fitted around the entire branch circumference and sealed by neutral silicone caulking. The limited external diameter of the foil collars minimized throughfall and rains accessing them. The RG3-M tipping-bucket rain gauges recorded the stemflow production and timing, thus computing the stemflow volume, duration, intensity and time lags to rain. The 0.5-cm-diameter polyvinyl chloride hoses channelled stemflow from the collars to the polyethylene film-covered gauges preventing throughfall and splash (Fig. 1). The hoses hung vertically to minimize the travel time to the rain gauges for an accurate recording of stemflow timing and intensity. These apparatuses were periodically checked to avoid leakages or blockages by insects and fallen leaves.

The stemflow variables at the branches of *C. korshinskii* and *S. psammophila* were calculated as follows.

(1) Stemflow volume (SFV, mL): the stemflow volume of individual branches of *C.*

korshinskii and *S. psammophila.* This variable was converted from the auto-recordings of branch stemflow via the tipping-bucket rain gauges (mm) by multiplying the base area of the RG3-M rain gauges (182.3 cm^2).

(2) Stemflow intensity ($mm \cdot h^{-1}$): the branch stemflow volume in a certain time, including SFI, SFI_{10} and SFI_i in this study. SFI and SFI_{10} are the average and 10-min maximum stemflow intensities during incident rains, which were computed by the branch stemflow as recorded by the tipping-bucket rain gauges (mm) and rainfall duration (h). SFI_i is the instantaneous stemflow intensity, which was calculated in terms of the tip volume of the RG3-M rain gauge (0.2 mm) and time intervals between neighbouring tips.

(3) Stemflow temporal dynamics: stemflow duration and time lags in response to rains.

SFD (h): the duration from stemflow beginning to its ending.

TLG (min): time lag of stemflow generation to rainfall beginning.

TLM (min): time lag of stemflow intensity peak to rainfall beginning.

TLE (min): time lag of stemflow ending to rainfall ceasing.

(4) Ratio of the intra-event stemflow intensity (RSFI, unitless): the ratio between stemflow intensity and rainfall intensity at 100-s intervals within events. Similar to the funnelling ratio (unitless) at the event scale (Herwitz, 1986; Siegert and Levia, 2014), the RSFI quantifies the convergence effect of stemflow by comparing stemflow intensity with rainfall intensity at a high temporal resolution (100 s) within events.

We calculated stemflow volume, intensity and temporal dynamics for 54 rainfall events

https://doi.org/10.5194/hess-2019-254
Preprint. Discussion started: 28 May 2019

during the experimental period. While representative rains had RAs of 5–10 mm, 10–20 mm and >20 mm, RSFI was compared during events to illustrate the fluctuating convergence effects of stemflow. The comparison between SFI_i and rainfall intensity depicted the synchronicity between stemflow and rains.

2.5 Data analysis

The stemflow variables were averaged among different BD categories to analyse the influences of rainfall characteristics on them. The Pearson correlation analyses tested the relationships between rainfall characteristics and stemflow variables. This analysis includes the intra-event rainfall characteristics (I, I_{10}, I_{b10}, I_{e10}, F, F_{10}, F_{b10} and F_{e10}) and stemflow variables (SFI, SFI_{10}, TLG, TLM and TLE), and the inter-event rainfall characteristics (RA, RD and RI) and stemflow variables (SFV and SFD). The significantly related factors were grouped according to the median value. These factors were then compiled into indicator matrices and standardized for a cross-tabulation check as required by a multiple correspondence analysis (MCA) (Levia et al., 2010; Van Stan et al., 2011, 2016). All qualified data were restructured into orthogonal dimensions (Hair et al., 1995), where distances between row and column points were maximized (Hill and Lewicki, 2007). As shown in the correspondence maps, rainfall feature clustering is tightly related to the centred stemflow variable. The most influential rainfall factor could then be identified with stepwise regression (Carlyle-Moses and Schooling, 2015). We built regression models in terms of the qualified level of significance (p<0.05) and the highest coefficient of determination (R^2). SPSS 21.0 (IBM Corporation, USA), Origin 8.5 (OriginLab Corporation, USA) and Excel 2019 (Microsoft Corporation, USA) were used for data

https://doi.org/10.5194/hess-2019-254
Preprint. Discussion started: 28 May 2019

analysis.

3 Results

3.1 Rainfall characteristics

Stemflow was automatically recorded for 54 rainfall events during the experimental period (Fig. 2). There were 20, 8, 10, 8, 4 and 4 rainfall events in the RA categories of ≤2 mm, 2–5 mm, 5–10 mm, 10–15 mm, 15–20 mm and >20 mm, respectively. The corresponding total RAs of the above five rainfall categories were 22.1 mm, 26.1 mm, 68.8 mm, 93.3 mm, 74.8 mm and 110.0 mm, respectively. The average I, I_{10}, I_{b10} and I_{e10} of the 54 rainfall events were 4.6±1.0 mm·h^{-1}, 11.5±2.1 mm·h^{-1}, 5.8±1.5 mm·h^{-1} and 2.9±0.7 mm·h^{-1}, respectively. The average F, F_{10}, F_{b10} and F_{e10} were 16.3±8.7 mg·m·s^{-1}, 25.7±9.6 mg·m·s^{-1}, 18.5±9.9 mg·m·s^{-1} and 15.8±7.0 mg·m·s^{-1}, respectively. RD and RI averaged 4.9±0.8 h and 50.9±6.1 h, respectively.

Rainfall events were further categorized in terms of rainfall-intensity peak amount, including Events A, B and C, with single, double and multiple peaks (17, 11 and 15 events, respectively) (Table 2). The remaining 11 events could not be categorized due to less than three intra-event recordings. Compared with Events A and B, Event C possessed significantly different rainfall characteristics, e.g., a larger RA (11.7 vs. 4.1 and 5.2 mm) and RD (10.3 vs. 2.5 and 3.6 h) but a smaller I_{10} (9.5 vs. 15.5 and 12.7 mm·h^{-1}), I_{b10} (2.8 vs. 7.7 and 9.9 mm·h^{-1}), I_{e10} (2.1 vs. 4.3 and 3.6 mm·h^{-1}), F_{10} (24.2 vs. 27.8 and 26.6 mg·m·s^{-1}), F_{b10} (15.4 vs. 19.7 and 21.7 mg·m·s^{-1}) and F_{e10} (13.4 vs. 17.3 and 16.6 mg·m·s^{-1}, respectively) (Table 2).

In general, the events were skewed in their distributions in terms of RA during the

https://doi.org/10.5194/hess-2019-254
Preprint. Discussion started: 28 May 2019

experimental period. The occurrences of events with a RA≤2 mm dominated the experimental period (40.7%), but the events with RAs>20 mm were the greatest contributor to the total RA (28.0%). However, a relatively equal distribution was noted during events with single (17 events), double (11 events) and multiple (15 events) rainfall-intensity peaks. In contrast, the multiple-intensity peak events had significantly larger rainfall amounts, durations, intensities and raindrop momentums (Table 2). Therefore, grouping events in terms of rainfall-intensity peak amounts was justified.

3.2 Stemflow volume, intensity and temporal dynamics

The stemflow variables of *C. korshinskii* and *S. psammophila* showed great inter-event variations during the experimental period (Fig. 3). *C. korshinskii* had larger SFV, SFI_{10}, SFD, TLG and TLE (1658.4±320.9 mL, 20.3±10.4 $mm \cdot h^{-1}$, 3.8±0.8 h, 66.2±10.6 min and 20.0±5.3 min, respectively) but significantly smaller TLM (109.4±20.5 min) and slightly smaller SFI (4.7±1.5 $mm \cdot h^{-1}$) than those of *S. psammophila* (1014.0±174.5 mL, 16.9±8.8 $mm \cdot h^{-1}$, 3.4±0.9 h, 54.8±11.7 min, 13.5±17.2 min, 120.5±22.1 min, 4.8±1.6 $mm \cdot h^{-1}$, respectively) (Table 3). The positive TLG, TLE and TLM indicated that both species generally started, maximized and ceased stemflow later than the rains.

As shown in Fig. 4, stemflow was well synchronized to rains with similar intensity peak shapes, amounts and positions for the two species. This result was demonstrated during representative events with different intensity peak amounts, including the rainfall events on July 17, 2015 (20.7 mm, Event A), on July 29, 2015 (7.3 mm, Event B), and on September 10, 2015 (13.3 mm, Event C). For these three events, *C. korshinskii* had larger RSFIs (2, 1.8 and 2.1, respectively) than those of *S. psammophila* (1.4, 0.9 and 1.4,

https://doi.org/10.5194/hess-2019-254
Preprint. Discussion started: 28 May 2019

respectively). Comparatively, the RSFI of *S. psammophila* fluctuated more dramatically around the value of 1.

Stemflow variables varied between rainfall event categories (Table 3). For Event C in comparison to Events A and B, *S. psammophila* had significantly larger SFV (2469.0 vs. 616.5 and 907.0 mL), SFD (8.2 vs. 1.2 and 3.4 h), TLM (235.8 vs. 64.3 and 93.4 min) and TLE (20.8 vs. 17.1 and 8.6 min) but significantly smaller SFI (2.4 vs. 7.2 and 6.0 mm·h^{-1}) and SFI_{10} (8.8 vs. 24.8 and 24.5 mm·h^{-1}, respectively). For Event C in comparison to Events A and B, *C. korshinskii* shared similar trends for its stemflow variables between event categories with those of *S. psammophila*, except for the slightly smaller TLE (18.5 vs. 22.3 and 18.7 min) and SFI (5.1 vs. 5.7 and 6.0 mm·h^{-1}, respectively).

3.3 Relationships between stemflow variables and rainfall characteristics

Correspondence had been established between rainfall characteristics and stemflow variables for *C. korshinskii* and *S. psammophila* (Fig. 5). These two species had similar correspondence patterns. As shown in Fig. 5, one-to-one correspondences were observed for SFV, SFD and TLE. The larger (or smaller) SFV, SFD and TLE corresponded to the larger (or smaller) RA, RD and RI, respectively. This result clearly demonstrated the dominant influences of RA, RD and RI on SFV, SFD and TLE, respectively. Nevertheless, one-to-more correspondences were noted for TLM, TLG, SFI and SFI_{10}. The larger TLM and TLG were, the smaller SFI and SFI_{10} were, and all corresponded to the smaller rainfall characteristics of I, I_{10}, I_{b10}, I_{e10}, F, F_{10}, F_{b10} and F_{e10}. In contrast, the smaller TLM and TLG were, the larger SFI and SFI_{10} were, and all corresponded to the larger rainfall characteristics of I, I_{10}, I_{b10}, I_{e10}, F, F_{10}, F_{b10} and F_{e10}. This result indicated that stemflow

https://doi.org/10.5194/hess-2019-254
Preprint. Discussion started: 28 May 2019

processes (SFI, SFI_{10}, TLG and TLM) were strongly affected by rainfall intensity and raindrop momentum. The rainfall characteristics influenced the stemflow variables at the corresponding temporal scales. This influence occurred at the inter-event scale between SFV and RA and SFD and RD, while this influence occurred at the intra-event scale for stemflow time lags (TLG and TLM) and intensities (SFI and SFI_{10}) with rainfall intensity (I, I_{10}, I_{b10} and I_{e10}) and raindrop momentum (F, F_{10}, F_{b10} and F_{e10}). The exception of mismatched temporal sales was noted between TLE and RI.

To identify the most influential rainfall characteristics affecting stemflow intensities and time lags, stepwise regression was performed and indicated that I_{10} significantly affected the TLM of both shrub species. For *C. korshinskii*, I, I_{10} and F were the most influential factors on SFI, SFI_{10} and TLG, respectively. However, for *S. psammophila*, F, F_{10} and F_{b10} significantly affected SFI, SFI_{10} and TLG, respectively. There were linear relationships between SFI and I (R^2=0.85, p<0.01) and SFI_{10} and I_{10} (R^2=0.90, p <0.01) for *C. korshinskii* and between SFD and RD for *C. korshinskii* (R^2=0.95, p<0.01) and *S. psammophila* (R^2=0.92, p<0.01) (Fig. 6). Moreover, power functional relations were found between SFI and F (R^2=0.82, p<0.01), SFI_{10} and F_{10} (R^2=0.90, p<0.01) (Fig. 6), TLG and F_{b10} (R^2=0.55, p<0.01) and TLM and I_{10} (R^2=0.40, p<0.01) (Fig. 7) for *S. psammophila*, and TLG and F (R^2=0.56, p <0.01) and TLM and I_{10} (R^2=0.38, p<0.01) (Fig. 7) for *C. korshinskii*. However, there was no significant quantitative relationship between TLE and RI for *C. korshinskii* (R^2=0.005, p=0.28) or *S. psammophila* (R^2=0.002, p=0.78) (Fig. 7).

4 Discussion

4.1 Stemflow intensity

Stemflow intensity is generally greater than rainfall intensity for different plant life forms. The xerophytic shrubs *C. korshinskii* and *S. psammophila* had larger average stemflow intensities than the average rainfall intensity (4.7±1.5 and 4.8±1.6 mm·h^{-1}, respectively, vs. 4.5±1.0 mm·h^{-1}) in this study. Broadleaf and coniferous species (*Quercus pubescens* Willd. and *Pinus sylvestris* L., respectively) also have larger average maximum stemflow intensities than the maximum rainfall intensity in north-eastern Spain (Cayuela et al., 2018). The gap between stemflow and rainfall intensity generally increased as the recording time intervals decreased. For *C. korshinskii* and *S. psammophila*, in comparison to I_{10} (10.9±2.1 mm·h^{-1}) at 10-min intervals, the SFI_{10} (20.3±10.4 and 16.9±8.8 mm·h^{-1}, respectively) was 1.5-fold greater. When recorded at 5-min intervals, SFI_5 (1232 mm·h^{-1}) is as much as 15-fold greater than rainfall intensity in the open tropical rainforest of Brazil (Germer et al., 2010). While calculating the dynamic time interval between neighbouring tips of the tipping-bucket rain gauges, SFI_i (240 mm·h^{-1}) was 3.3-fold greater than the corresponding rainfall intensity (72 mm·h^{-1}). Therefore, stemflow recorded at a higher temporal resolution provided more information into the dynamic nature of stemflow and real-time responses to rainfall characteristics within events.

Greater stemflow intensity than rainfall intensity is hydrologically significant in terrestrial ecosystems. This scenario indicates the convergence of the canopy-intercepted rains into the limited area around the trunk or branch bases within a certain time period. The funnelling ratio, which quantifies the efficiency of individual plants in capturing and delivering raindrops at an event scale (Siegert and Levia, 2014), is commonly applied to assess the convergence effect (Herwitz, 1986; Wang et al., 2013; Fan et al., 2015). If the funnelling ratio is greater than 1, then more water is collected at the trunk or branch base than at the clearings during incident rains. However, the process to assess the convergence effect of stemflow within events has still not been adequately studied.

RSFI depicted the intra-event convergence effects of stemflow by comparing stemflow and rainfall intensities at 100-s intervals starting from the beginning to the ending of incident rains. We found that RSFI fluctuated around the value of 1 for both shrub species (Fig. 4). The RSFI was generally greater than 1 for *C. korshinskii*, whereas the RSFI for *S. psammophila* fluctuated more dramatically. This result indicated that comparatively more rainwater was delivered within a short period to the branch base of *C. korshinskii* during the rain process. This result agreed with the results of reports related to the more efficient stemflow production of *C. korshinskii* at the event scale, as expressed by its larger stemflow productivity (1.95 $mL \cdot g^{-1}$) and funnelling ratio (173.3) than those of *S. psammophila* (1.19 $mL \cdot g^{-1}$ and 69.3, respectively) (Yuan et al., 2017). Therefore, RSFI demonstrated the process-based estimation of stemflow efficiency. Carlyle-Moses et al. (2018) have addressed the importance of studying stemflow convergence effects by employing the funnelling ratio at the stand scale. We highly recommended that future studies evaluate convergence effects during rain events by combining the results of the funnelling ratio and RSFI.

4.2 Stemflow temporal dynamics

Stemflow was well synchronized to the rains. This result agreed with those of Levia et al. (2010), who demonstrated a marked synchronicity between stemflow volume and RA in 5-min intervals for *Fagus. grandifolia*. The duration and time lags to rains were critical to describe stemflow temporal dynamics. Our results indicated that in comparison to *S. psammophila*, *C. korshinskii* takes a longer time to initiate (66.2 vs. 54.8 min), end (20.0 vs. 13.5 min) and produce stemflow (3.8 vs. 3.4 h) but a shorter time to maximize stemflow (109.4 vs. 120.5 min, respectively). Moreover, the TLMs of both shrub species were in the range of the TLMs for *S. psammophila* (20–210 min) in the Mu Us desert of China (Yang, 2010).

Varying TLGs were documented for different species. Approximately 15 min, 1 h and 1.5 h are needed to initiate the stemflow of palms (Germer, 2010), pine trees and oak trees (Cayuela et al., 2018), respectively. In addition, an almost instantaneous start of stemflow has also observed as rain began for *Quercus rubra* (Durocher, 1990), *Fagus grandifolia* and *Liriodendron tulipifera* (Levia et al., 2010). In contrast to the positive TLE dominating xerophytic shrubs, the TLE greatly varies with tree species. TLE is as much as 48 h for Douglas fir, oak and redwood in California, USA (Reid and Levia, 2009), and almost 11 h for palm trees in Brazil (Germer, 2010). However, for sweet chestnut and oak, almost no stemflow continues when rains cease in Bristol, England (Durocher, 1990). These scenarios might occur due to the sponge effect of the canopy surface (Germer, 2010), which buffers stemflow generation, maximization and cessation before saturation. These conclusions were consistent with the smaller stemflow intensities of *C. korshinskii* and *S. psammophila* than the rainfall intensity when rain began, as part of the rains was used to wet canopies (Fig. 4). The hydrophobic bark traits benefit stemflow initiation with limited time lags to rains. In contrast, the hydrophilic bark traits are conducive for continuing stemflow after rain stops, which keep the preferential flow paths wetter for longer time periods (Levia and

Germer, 2015). As a result, it takes time to transfer intercepted rains from the leaf, branch and trunk to the base. This process strongly affects the stemflow volume, intensity and loss as evaporation.

The dynamics of intra-event rainfall intensity complicates the stemflow time lags to rains. A 1-h lag to begin and stop stemflow with the beginning and ending of rains was observed for ashe juniper trees during high-intensity events, but no stemflow was generated at low-intensity storms (Owens et al., 2006). Rainfall intensity was an important dynamic rainfall characteristic affecting stemflow volume. Owens et al. (2006) found the most significant difference between various rainfall intensities located in the stemflow patterns other than throughfall and interception loss. During events with a front-positioned, single rainfall-intensity peak, *S. psammophila* maximized stemflow in a shorter time than *C. korshinskii* did in the Mu Us desert (30 and 50 min) (Yang, 2010). During these events, a smaller SFD (1.5 h) and a larger TLE (55.8 min) and SFI (11.5 mm·h^{-1}) were also observed for *C. korshinskii* than for *S. psammophila* in this study. This result highlighted the amounts and occurrence time of rainfall-intensity peak affecting the stemflow process, which was consistent with the finding of Dunkerley (2014).

Raindrops presented rainfall characteristics at finer temporal-spatial scales. They are usually ignored because rains were generally regarded as a continuum rather than a discrete process consisting of individual raindrops of various sizes, velocities, inclination angles and kinetic energies. Raindrops hit the canopy surface and create splashes at different canopy layers (Bassette and Bussière, 2008; Li et al., 2016). This process accelerates canopy wetting and increases the water supply for stemflow production. Therefore,

https://doi.org/10.5194/hess-2019-254
Preprint. Discussion started: 28 May 2019

raindrop momentum was introduced in this study to represent the comprehensive effects of raindrop attributes. Our results indicated that raindrop momentum was sensitive to predicting the variations in stemflow intensity and temporal dynamics with significant linear or power functional relations (Figs. 6 and 7). Compared with the importance of rainfall intensity for *C. korshinskii*, raindrop momentum more significantly affected the stemflow process of *S. psammophila*. This result might be related to the larger canopy size and height of *S. psammophila* (21.4±5.2 m^2 and 3.5±0.2 m) than that of *C. korshinskii* (5.1±0.3 m^2 and 2.1±0.2 m, respectively). Thus, more layers are available within canopies to intercept the splashes created by raindrop striking (Bassette and Bussière, 2008; Li et al., 2016), thus shortening the paths and having more water supply for stemflow production.

4.3 Temporal-dependent influence of rainfall characteristics

This study discussed stemflow variables and rainfall characteristics at different temporal scales. Stemflow variables were further categorized into volume, intensity and temporal dynamics. The last two variables depicted the stemflow process with a high temporal resolution. The influences of rainfall characteristics were explored at a fine temporal scale by introducing raindrop momentum, rainfall-intensity peak amounts and intra-event positions. We found that rainfall characteristics affected stemflow variables at the corresponding temporal scales. RA and RD controlled SFV and SFD, respectively, at the inter-event scale. However, stemflow intensity (e.g., SFI and SFI_{10}) and temporal dynamics (e.g., TLG and TLM) were strongly influenced by rainfall intensity (e.g., I, I_{10} and I_{b10}) and raindrop momentum (e.g., F, F_{10} and F_{b10}) at the intra-event scales. These results were verified by the well-fitting linear or power functional equations among them

https://doi.org/10.5194/hess-2019-254
Preprint. Discussion started: 28 May 2019

(Figs. 6 and 7). Furthermore, the influences of rainfall intensity and raindrop momentum on stemflow process were species-specific. In contrast to the significance of rainfall intensity on the stemflow process of *C. korshinskii*, raindrop momentum imposed a greater influence on the stemflow process of *S. psammophila*.

In general, rainfall characteristics had temporal-dependent influences on the corresponding stemflow variables. The only exception was found between TLE and RI. RI tightly corresponded to TLE for both species tested by the MCA, but there was no significant quantitative relationship between them (R^2=0.005, p=0.28 for *C. korshinskii*, and R^2=0.002, p=0.78 for *S. psammophila*). This result might be related to the mismatched temporal scales between TLE and RI. TLE represented stemflow temporal dynamics at the intra-event scale, while RI was the interval times between neighbouring rains at the inter-event scale. The mismatched temporal scales might also partly explain the long-standing debates on the controversial positive, negative and even no significant influences of rainfall intensity (depicting raining process at 5 min, 10 min, 60 min, etc.) on event-based stemflow volume (Owens et al., 2006; André et al., 2008; Zhang et al., 2015).

5 Conclusions

Stemflow intensity and temporal dynamics are important in depicting the stemflow process and its interactions with rainfall characteristics within events. We categorized stemflow variables into the volume, intensity and temporal dynamics, thus representing the stemflow yield and process at different temporal scales. The influences of rainfall characteristics were quantified at a fine temporal scale by introducing SFI_i, RSFI, raindrop momentum, rainfall-intensity peak amounts and intra-event positions. The results indicated

https://doi.org/10.5194/hess-2019-254
Preprint. Discussion started: 28 May 2019

Hydrology and Earth System Sciences Discussions

that rainfall characteristics had temporal-dependent influences on stemflow variables. RA and RD controlled SFV and SFD at the inter-event scale. Rainfall intensity and raindrop momentum significantly affected stemflow intensity and time lags to rains at the intra-event scale except for TLE. Although there was tight correspondence between TLE and RI by MCA, there was no significant quantitative relationship (R^2<0.005, p>0.28) due to the mismatched temporal scale between them. These findings advance our understanding of the stemflow process and its influential mechanism and help model the critical process-based hydrological fluxes of terrestrial ecosystems.

Data availability. The data collected in this study are available upon request to the authors.

Author contributions. GYG and CY set up the research goals and designed field experiments. CY measured and analyzed the data. GYG and BJF provided the financial support for the experiments, and supervised the execution. CY created the figures and wrote the original draft. GYG, BJF, DMH, XWD and XHW reviewed and edited the draft in serval rounds of revision.

Competing interests. The authors declare that they have no conflict of interest.

Acknowledgements. This research was sponsored by the National Natural Science Foundation of China (nos. 41390462 and 41822103), the National Key Research and Development Program of China (no. 2016YFC0501602), the Chinese Academy of

Sciences (no. QYZDY-SSW-DQC025), the Youth Innovation Promotion Association CAS (no. 2016040), and the China Postdoctoral Science Foundation (no. 2018M633427). We appreciate Prof. D. F. Levia in University of Delaware for reviewing and improving this manuscript. Thanks to Liwei Zhang for the catchment GIS mapping. Special thanks are given to Shenmu Erosion and Environment Research Station for experimental support to this research.

References

André, F., Jonard, M. and Ponette, Q.: Influence of species and rain event characteristics on stemflow volume in a temperate mixed oak-beech stand, Hydrol. Process., 22, 4455–4466. https://doi.org/10.1002/hyp.7048, 2008.

Bassette, C. and Bussière, F.: Partitioning of splash and storage during raindrop impacts on banana leaves, Agr., Forest Meteorol., 148, 991–1004, https://doi.org/10.1016/j.agrformet.2008.01.016, 2008.

Bittar, T.B., Pound, P., Whitetree, A., Moore, L.D. and Van Stan John, T.: Estimation of throughfall and stemflow bacterial flux in a subtropical oak-cedar forest. Geophys. Res. Lett., 45, 1410–1418, https://doi.org/10.1002/2017GL075827, 2018.

Brandt, C.J.: Simulation of the size distribution and erosivity of raindrops and throughfall drops. Earth. Surf. Proc. Land., 15, 687–698, https://doi.org/10.1002/esp.3290150803, 1990.

Bundt, M., Widmer, F., Pesaro, M., Zeyer, J. and Blaser, P.: Preferential flow paths: biological 'hot spots' in soils. Soil. Biol. Biochem., 33, 729–738, https://doi.org/10.1016/S0038-0717(00)00218-2, 2001.

Carlyle-Moses, D.E., Iida, S.I., Germer, S., Llorens, P., Michalzik, B., Nanko, K., Tischer, A. and Levia, D.F.: Expressing stemflow commensurate with its ecohydrological importance, Adv. Water Resources, 121, 472–479, https://doi.org/10.1016/j.advwatres.2018.08.015, 2018.

Carlyle-Moses, D.E. and Price, A.G.: Growing-season stemflow production within a deciduous forest of southern Ontario, Hydrol. Process., 20, 3651–3663, https://doi.org/10.1002/hyp.6380, 2006.

Carlyle-Moses, D.E. and Schooling, J.: Tree traits and meteorological factors influencing the initiation and rate of stemflow from isolated deciduous trees, Hydrol. Process., 29, 4083–4099, https://doi.org/10.1002/hyp.10519, 2015.

Cayuela, C., Llorens, P., Sánchez-Costa, E., Levia, D.F. and Latron, J.: Effect of biotic and abiotic factors on inter- and intra-event variability in stemflow rates in oak and pine stands in a Mediterranean mountain area, J. Hydrol., 560, 396–406, https://doi.org/10.1016/j.jhydrol.2018.03.050, 2018.

Dawoe, E.K., Barnes, V.R. and Oppong, S.K.: Spatio-temporal dynamics of gross rainfall partitioning and nutrient fluxes in shaded-cocoa (*Theobroma cocoa*) systems in a tropical semi-deciduous forest, Agroforst. Syst., 92, 397–413, https://doi.org/10.1007/s10457-017-0108-3, 2018.

Dunkerley, D.L.: Stemflow on the woody parts of plants: dependence on rainfall intensity and event profile from laboratory simulations, Hydrol. Process., 28, 5469–5482, https://doi.org/10.1002/hyp.10050, 2014.

https://doi.org/10.5194/hess-2019-254
Preprint. Discussion started: 28 May 2019

Dunkerley, D.L.: Rainfall intensity bursts and the erosion of soils: an analysis highlighting the need for high temporal resolution rainfall data for research under current and future climates, Earth Surf. Dynam., 7, 345–360, https://doi.org/10.5194/esurf-7-345-2019, 2019.

Durocher, M.G.: Monitoring spatial variability of forest interception, Hydrol. Process., 4, 215–229, https://doi.org/10.1002/hyp.3360040303, 1990.

Fan, J.L., Baumgartl, T., Scheuermann, A. and Lockington, D.A.: Modeling effects of canopy and roots on soil moisture and deep drainage. Vadose. Zone. J., 14, 1–18, https://doi.org/10.2136/vzj2014.09.0131, 2015.

Firn, R.: Plant intelligence: an alternative point of view, Ann. Bot., 93, 345–351, https://doi.org/10.1093/aob/mch058, 2004.

Garbelotto, M.M., Davidson, J.M., Ivors, K., Maloney, P.E., Hüberli, D., Koike, S.T. and Rizzo, D.M.: Non-oak native plants are main hosts for sudden oak death pathogen in California, Calif. Agric, 57, 18–23, https://doi.org/10.3733/ca.v057n01p18, 2003.

Giacomin, A. and Trucchi, P.: Rainfall interception in a beech coppice (Acquerino, Italy). J. Hydrol., 137, 141–147, https://doi.org/10.1016/0022-1694(92)90052-W, 1992.

Germer, S., Werther, L. and Elsenbeer, H.: Have we underestimated stemflow? Lessons from an open tropical rainforest, J. Hydrol., 395, 169–179, https://doi.org/10.1016/j.jhydrol.2010.10.022, 2010.

Hair, J.F., Anderson, R.E., Tatham, R.L. and Black, W.C.: Multivariate Data Analysis, fourth ed. Prentice Hall College Division, 745 p, 1995.

Herwitz, S.R.: Infiltration-excess caused by Stemflow in a cyclone-prone tropical rainforest,

https://doi.org/10.5194/hess-2019-254
Preprint. Discussion started: 28 May 2019

Hydrology and Earth System Sciences
Open Access
Discussions

Earth Surf. Proc. Land, 11, 401–412, https://doi.org/10.1002/esp.3290110406, 1986.

Herwitz, S.R. and Slye, R.E.: Three-dimensional modeling of canopy tree interception of wind-driven rainfall, J. Hydrol., 168, 1–4, https://doi.org/10.1016/0022-1694(94)02643-P, 1995.

Hill, T. and Lewicki, P.: Statistics: Methods and Applications. Statsoft, Tulsa, 800 p, 2007.

Iida, S.I., Levia, D.F., Shimizu, A., Shimizu, T., Tamai, K., Nobuhiro, T., Kabeya, N., Noguchi, S., Sawano, S. and Araki, M.: Intrastorm scale rainfall interception dynamics in a mature coniferous forest stand, J. Hydrol., 548, 770–783, https://doi.org/10.1016/j.jhydrol.2017.03.009, 2017.

Jia, X.X., Shao, M.A., Wei, X.R. and Wang, Y. Q.: Hillslope scale temporal stability of soil water storage in diverse soil layers, J. Hydrol., 498, 254–264, https://doi.org/10.1016/j.jhydrol.2013.05.042, 2013.

Johnson, M.S. and Lehmann, J.: Double-funneling of trees: Stemflow and root-induced preferential flow, Ecoscience, 13, 324–333, https://doi.org/0.2980/i1195-6860-13-3-324.1, 2006.

Kéfi, S., Rietkerk, M., Alados, C.L., Pueyo, Y., Papanastasis, V.P., ElAich, A. and De Ruiter, P.C.: Spatial vegetation patterns and imminent desertification in Mediterranean arid ecosystems, Nature, 449, 213–217, https://doi.org/10.1038/nature06111, 2007.

Kimble, P.D.: Measuring the momentum of throughfall drops and raindrops. Master Thesis. Western Kentucky University, Bowling Green, 126 pp, 1996.

Levia, D.F. and Germer, S.: A review of stemflow generation dynamics and stemflow-environment interactions in forests and shrublands, Rev. Geophys., 53, 673-

714, 2015, https://doi.org/10.1002/2015RG000479, 2015.

Levia, D.F., Van Stan, J.T., Mage, S.M. and Kelley-Hauske, P.W.: Temporal variability of stemflow volume in a beech-yellow poplar forest in relation to tree species and size, J. Hydrol., 380, 112–120, https://doi.org/10.1016/j.jhydrol.2009.10.028, 2010.

Li X., Xiao, Q.F., Niu, J.Z., Dymond, S., van Doorn, N.S., Yu, X.X., Xie, B.Y., Lv, X.Z., Zhang, K.B. and Li, J.: Process-based rainfall interception by small trees in Northern China: The effect of rainfall traits and crown structure characteristics, Agric. For. Meteorol., 218–219, 65–73, https://doi.org/10.1016/j.agrformet.2015.11.017, 2016.

Li, X.Y., Liu, L.Y., Gao, S.Y., Ma, Y.J. and Yang, Z.P.: Stemflow in three shrubs and its effect on soil water enhancement in semiarid loess region of China, Agric. For. Meteorol., 148, 1501–1507, https://doi.org/10.1016/j.agrformet.2008.05.003, 2008.

Magliano, P.N., Whitworth-Hulse, J.I. and Baldi, G.: Interception, throughfall and stemflow partition in drylands: Global synthesis and meta-analysis, J. Hydrol., 568, 638–645, https://doi.org/10.1016/j.jhydrol.2018.10.042, 2019.

Martinez-Meza, E. and Whitford, W.: Stemflow, throughfall and channelization of stemflow by roots in three Chihuahuan desert shrubs, J. Arid Environ., 32, 271–287, https://doi.org/10.1006/jare.1996.0023, 1996.

Mcclain, M.E., Boyer, E.W., Dent, C.L., Gergel, S.E., Grimm, N.B., Groffman, P.M., Hart, S.C., Harvey, J.W., Johnston, C.A. and Mayorga, E.: Biogeochemical hot spots and hot moments at the interface of terrestrial and aquatic ecosystems, Ecosystems, 6, 301–312, https://doi.org/10.1007/s10021-003-0161-9, 2003.

Návar, J.: Stemflow variation in Mexico's northeastern forest communities: Its contribution to soil moisture content and aquifer recharge, J. Hydrol., 408, 35–42, https://doi.org/10.1016/j.jhydrol.2011.07.006, 2011.

Owens, M.K., Lyons, R.K. and Alejandro, C.L.: Rainfall partitioning within semiarid juniper communities: effects of event size and canopy cover, Hydrol. Process., 20, 3179–3189, https://doi.org/10.1002/hyp.6326, 2006.

Reid, L.M. and Lewis, J.: Rates, timing, and mechanisms of rainfall interception loss in a coastal redwood forest, J. Hydrol., 375, 459–470, https://doi.org/10.1016/j.jhydrol.2009.06.048, 2009.

Siegert, C.M. and Levia, D.F.: Seasonal and meteorological effects on differential stemflow funneling ratios for two deciduous tree species, J. Hydrol., 519, 446–454, https://doi.org/10.1016/j.jhydrol.2014.07.038, 2014.

Spencer, S.A. and van Meerveld, H.J.: Double funnelling in a mature coastal British Columbia forest: spatial patterns of stemflow after infiltration, Hydrol. Process., 30, 4185–4201, https://doi.org/10.1002/hyp.10936, 2016.

Staelens, J., De Schrijver, A., Verheyen, K. and Verhoest N.E.: Rainfall partitioning into throughfall, stemflow, and interception within a single beech (*Fagus sylvatica* L.) canopy: influence of foliation, rain event characteristics, and meteorology, Hydrol. Process., 22, 33–45, https://doi.org/10.1002/hyp.6610, 2008.

Teachey, M.E., Pound, P., Ottesen, E.A. and Van Stan, J.T.: Bacterial community composition of throughfall and stemflow, Front. Plant. Sci., 1, 1–6, https://doi.org/10.3389/ffgc.2018.00007, 2018.

Uijlenhoet, R. and Sempere Torres, D.: Measurement and parameterization of rainfall

https://doi.org/10.5194/hess-2019-254
Preprint. Discussion started: 28 May 2019

Hydrology and Earth System Sciences
Discussions

microstructure, J. Hydrol., 328, 1, 1–7, https://doi.org/10.1016/j.jhydrol.2005.11.038, 2006.

Van Stan, J.T. and Levia, D.F.: Inter- and intraspecific variation of stemflow production from *Fagus grandifolia* Ehrh. (American beech) and *Liriodendron tulipifera* L. (yellow poplar) in relation to bark microrelief in the eastern United States, Ecohydrology, 3, 11–19, https://doi.org/10.1002/eco.83, 2010.

Van Stan, J.T., Siegert, C.M., Levia D.F. and Scheick, C.E.: Effects of wind-driven rainfall on stemflow generation between codominant tree species with differing crown characteristics, Agric. For. Meteorol., 151, 9, 1277–1286, https://doi.org/10.1016/j.agrformet.2011.05.008, 2011.

Van Stan, J.T., Gay, T.E. and Lewis, E.S.: Use of multiple correspondence analysis (MCA) to identify interactive meteorological conditions affecting relative throughfall, J. Hydrol., 533, 452–460, https://doi.org/10.1016/j.jhydrol.2015.12.039, 2016.

Wang, X.P., Wang, Z.N., Berndtsson, R., Zhang, Y.F. and Pan, Y.X.: Desert shrub stemflow and its significance in soil moisture replenishment, Hydrol. Earth Syst. Sci., 15, 561–567, https://doi.org/10.5194/hess-15-561-2011, 2011.

Wang, X.P., Zhang, Y.F., Wang, Z.N., Pan, Y.X., Hu, R., Li, X.J. and Zhang, H.: Influence of shrub canopy morphology and rainfall characteristics on stemflow within a revegetated sand dune in the Tengger Desert, NW China, Hydrol. Process., 27, 1501–1509, https://doi.org/10.1002/hyp.9767, 2013.

Yang, Z.P.: Rainfall partitioning process and its effects on soil hydrological processes for sand-fixed shrubs in Mu us sandland, Northwest China. PhD Thesis. Beijing Normal

https://doi.org/10.5194/hess-2019-254
Preprint. Discussion started: 28 May 2019

University, Beijing, 123 pp (in Chinese with English abstract), 2010.

Yang, X.L., Shao, M.A. and Wei, X.H.: Stemflow production differ significantly among tree and shrub species on the Chinese Loess Plateau, J. Hydrol., 568, 427–436, https://doi.org/10.1016/j.jhydrol.2018.11.008, 2019.

Yuan, C., Gao, G.Y. and Fu, B.J.: Stemflow of a xerophytic shrub (*Salix psammophila*) in northern China: Implication for beneficial branch architecture to produce stemflow, J. Hydrol., 539, 577–588, https://doi.org/10.1016/j.jhydrol.2016.05.055, 2016.

Yuan, C., Gao, G.Y. and Fu, B.J.: Comparisons of stemflow and its bio-/abiotic influential factors between two xerophytic shrub species, Hydrol. Earth Syst. Sci., 21, 1421–1438, https://doi.org/10.5194/hess-21-1421-2017, 2017.

Zabret, K., Rakovec, J. and Šraj, M.: Influence of meteorological variables on rainfall partitioning for deciduous and coniferous tree species in urban area, J. Hydrol., 558, 29–41, https://doi.org/10.1016/j.jhydrol.2018.01.025, 2018.

Zhang, Y.F., Wang X.P., Hu, R., Pan Y.X. and Paradeloc, M.: Rainfall partitioning into throughfall, stemflow and interception loss by two xerophytic shrubs within a rain-fed re-vegetated desert ecosystem, northwestern China, J. Hydrol., 527, 1084–1095, https://doi.org/10.1016/j.jhydrol.2015.05.060, 2015

https://doi.org/10.5194/hess-2019-254
Preprint. Discussion started: 28 May 2019

Table 1. Branch morphologies of *C. korshinskii* and *S. psammophila* for stemflow recording.

Shrub species	BD categories (mm)	Amount	BD (mm)	BL (cm)	BA (°)
	5–10	2	6.6	131	61
	10–15	2	13.1	168	43
C. korshinskii	15–18	2	17.8	206	72
	18–25	1	22.1	242	50
	>25	NA	NA	NA	NA
	5–10	2	7.5	248	69
	10–15	2	13.2	343	80
S. psammophila	15–18	NA	NA	NA	NA
	18–25	2	21.8	286	76
	>25	1	31.3	356	60

Notes: BD, BL and BA are branch basal diameter, length and inclination angle, respectively. NA means not applicable.

https://doi.org/10.5194/hess-2019-254
Preprint. Discussion started: 28 May 2019

Hydrology and Earth System Sciences
Open Access
Discussions

Table 2. Rainfall characteristics during events with different intensity peak amounts.

Indicators	Event A	Event B	Event C	Others	Average
RA (mm)	4.1	5.2	11.7	0.6	5.4 ± 0.9
RD (h)	2.5	3.6	10.3	2.2	4.7 ± 0.8
RI (h)	48.5	70.5	57.3	26.1	50.6 ± 6.1
I ($mm \cdot h^{-1}$)	5.6	5.5	4.6	2.2	4.5 ± 1.0
I_{10} ($mm \cdot h^{-1}$)	15.5	12.7	9.5	6.0	10.9 ± 2.1
I_{b10} ($mm \cdot h^{-1}$)	7.7	9.9	2.8	1.6	5.5 ± 1.4
I_{e10} ($mm \cdot h^{-1}$)	4.3	3.6	2.1	1.2	2.8 ± 0.7
F ($mg \cdot m \cdot s^{-1}$)	17.1	17.6	17.2	12.5	16.1 ± 1.2
F_{10} ($mg \cdot m \cdot s^{-1}$)	27.8	26.6	24.2	21	24.9 ± 1.4
F_{b10} ($mg \cdot m \cdot s^{-1}$)	19.7	21.7	15.4	16.9	18.4 ± 1.4
F_{e10} ($mg \cdot m \cdot s^{-1}$)	17.3	16.6	13.4	16.8	16.0 ± 1.0

Note: Event A, Event B and Event C are events with the single, double and multiple rainfall intensity peaks, respectively, and Others are events excluded from the categorization. RA is the rainfall amount. RD and RI are rainfall duration and interval, respectively. I and I_{10} are the average and 10-min maximum rainfall intensity, respectively. I_{b10} and I_{e10} are the average rainfall intensity in 10 min after rain beginning and before rain ending, respectively. F and F_{10} are the average and 10-min maximum raindrop momentum, respectively. F_{b10} and F_{e10} are the average raindrop momentum in 10 min after rain beginning and before rain ending, respectively.

670 **Table 3.** Stemflow variables of *C. korshinskii* and *S. psammophila* during rainfall events with
671 different intensity peak amounts.

Species	Stemflow variables	Event A	Event B	Event C	Others	Average
C. korshinskii	SFV (mL)	934.1	1552.5	3719.7	67.3	1658.4 ± 320.9
	SFI ($mm{\cdot}h^{-1}$)	5.7	6.0	5.1	1.9	4.7 ± 1.5
	SFI_{10} ($mm{\cdot}h^{-1}$)	30.2	26.4	15.3	9.1	20.3 ± 10.4
	TLG (min)	67.3	56.2	67.0	74.2	66.2 ± 10.6
	TLE (min)	22.3	18.7	18.5	20.6	20.0 ± 5.3
	TLM (min)	81.1	75.5	202.1	78.8	109.4 ± 20.5
	SFD (h)	1.4	3.1	9.1	1.4	3.8 ± 0.8
S. psammophila	SFV (mL)	616.5	907.0	2469.0	63.4	1014.0 ± 174.5
	SFI ($mm{\cdot}h^{-1}$)	7.2	6.0	2.4	3.4	4.8 ± 1.6
	SFI_{10} ($mm{\cdot}h^{-1}$)	24.8	24.5	8.8	9.4	16.9 ± 8.8
	TLG (min)	84.9	46.5	56.1	31.5	54.8 ± 11.7
	TLE (min)	17.1	8.6	20.8	7.3	13.5 ± 17.2
	TLM (min)	64.3	93.4	235.8	88.4	120.5 ± 22.1
	SFD (h)	1.2	3.4	8.3	0.7	3.4 ± 0.9

672 Note: Event A, Event B and Event C are events with the single, double and multiple rainfall intensity peaks,
673 respectively, and Others are events excluded from the categorization. TLG and TLM are the time lags of
674 stemflow generating and maximizing to begin of rainfall, respectively. TLE is the time lag of stemflow ending
675 to cease of rainfall. SFD is the stemflow duration. SFV is the stemflow volume. SFI is the average stemflow
676 intensity. SFI_{10} is the maximum stemflow intensity in 10 min.

https://doi.org/10.5194/hess-2019-254
Preprint. Discussion started: 28 May 2019

Hydrology and Earth System Sciences
Discussions

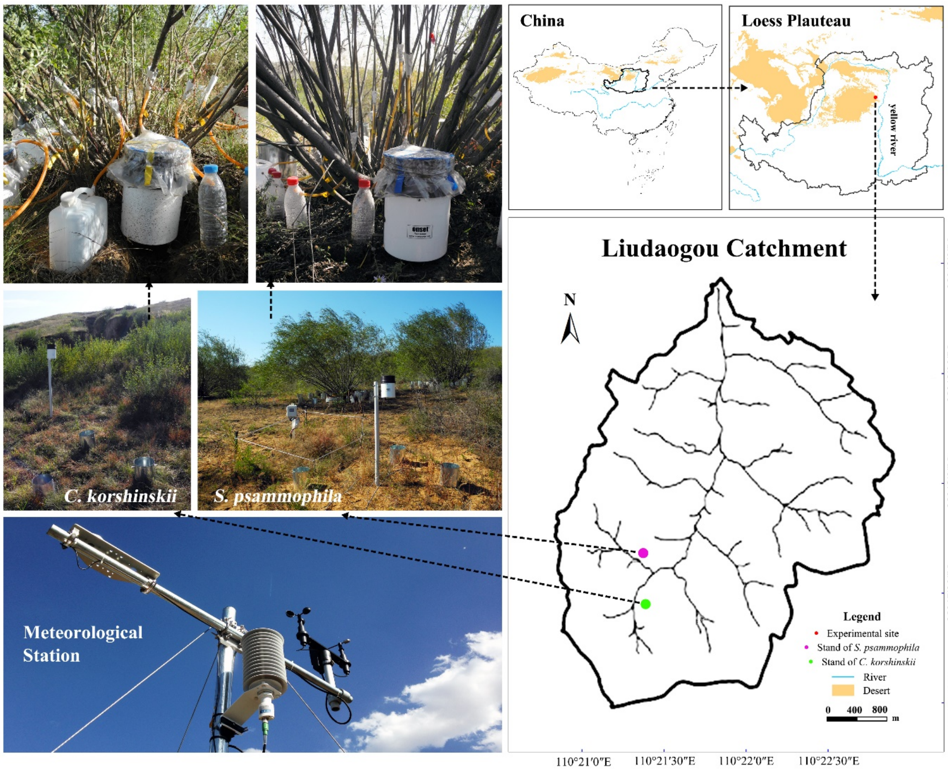

Figure 1. Locations and experimental settings in the plots of *C. korshinskii* and *S. psammophila*.

https://doi.org/10.5194/hess-2019-254
Preprint. Discussion started: 28 May 2019

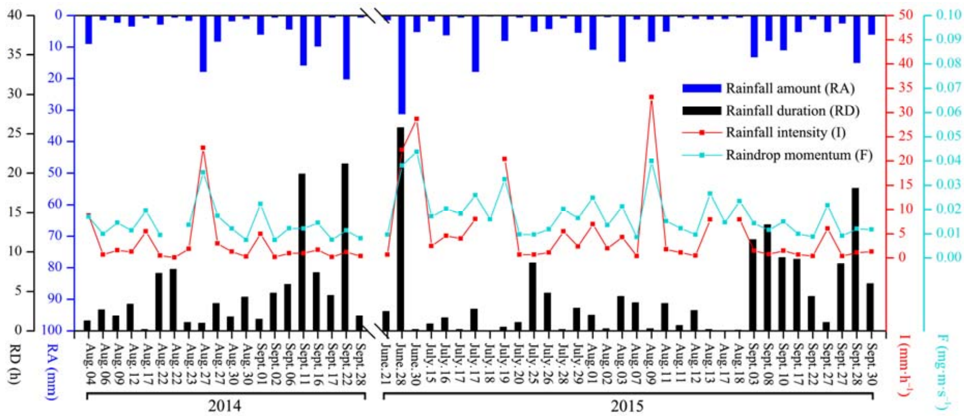

Figure 2. Inter-event variations in rainfall characteristics during the experimental period.

https://doi.org/10.5194/hess-2019-254
Preprint. Discussion started: 28 May 2019

682

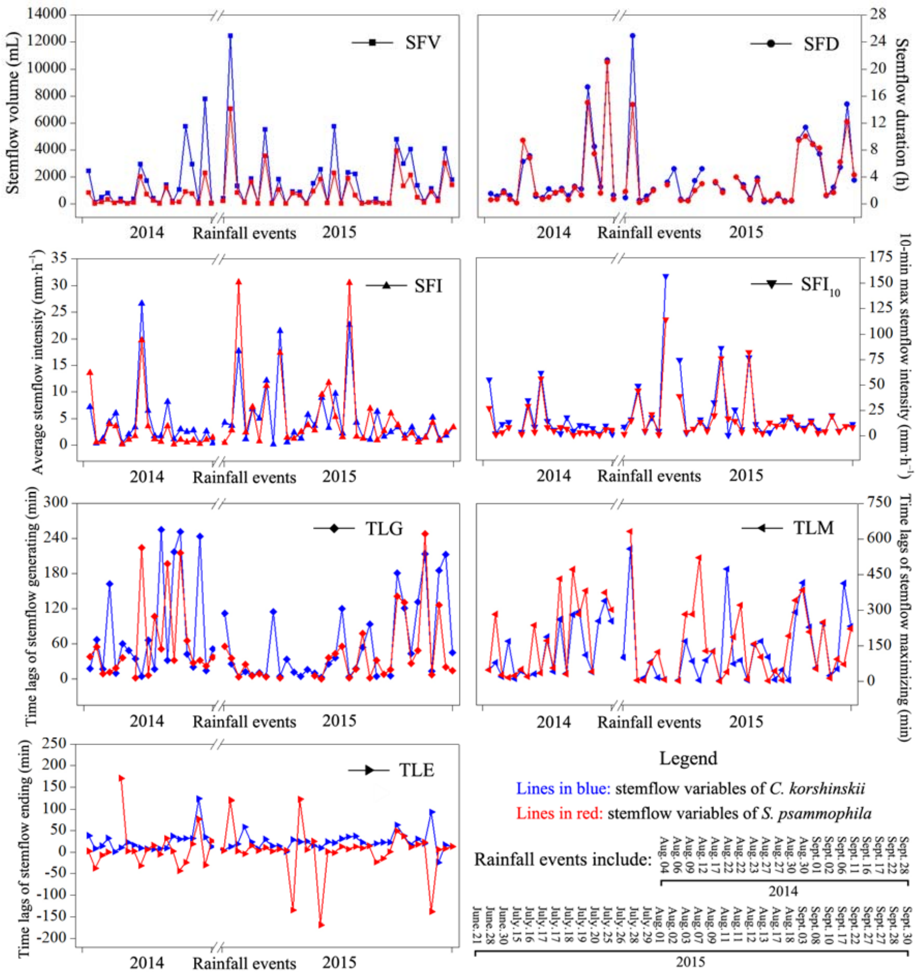

683 **Figure 3.** Inter-event variations in stemflow variables of *C. korshinskii* and *S. psammophila*

684 during the experimental period.

https://doi.org/10.5194/hess-2019-254
Preprint. Discussion started: 28 May 2019

Hydrology and Earth System Sciences
Open Access
EGU
Discussions

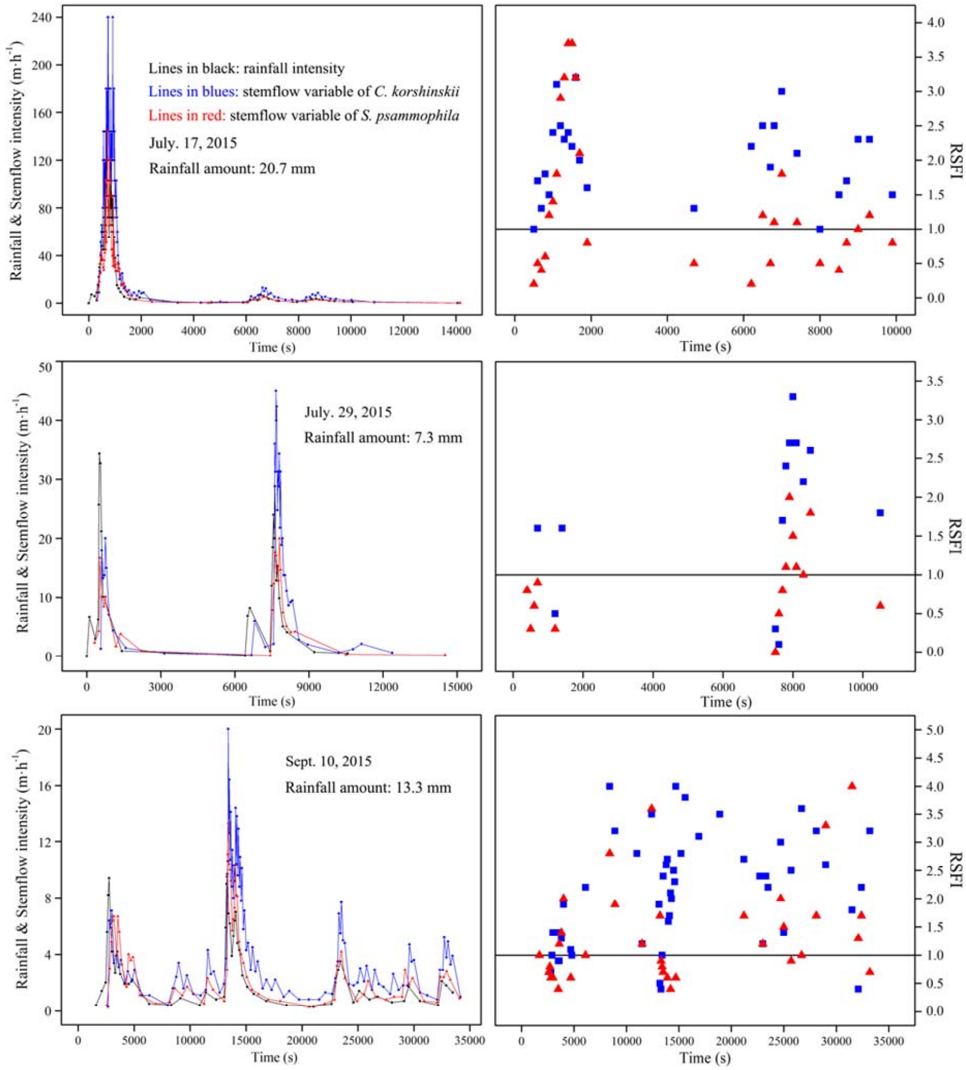

Figure 4. Stemflow synchronicity of *C. korshinskii* and *S. psammophila* to rains during representative events with different rainfall-intensity peaks.

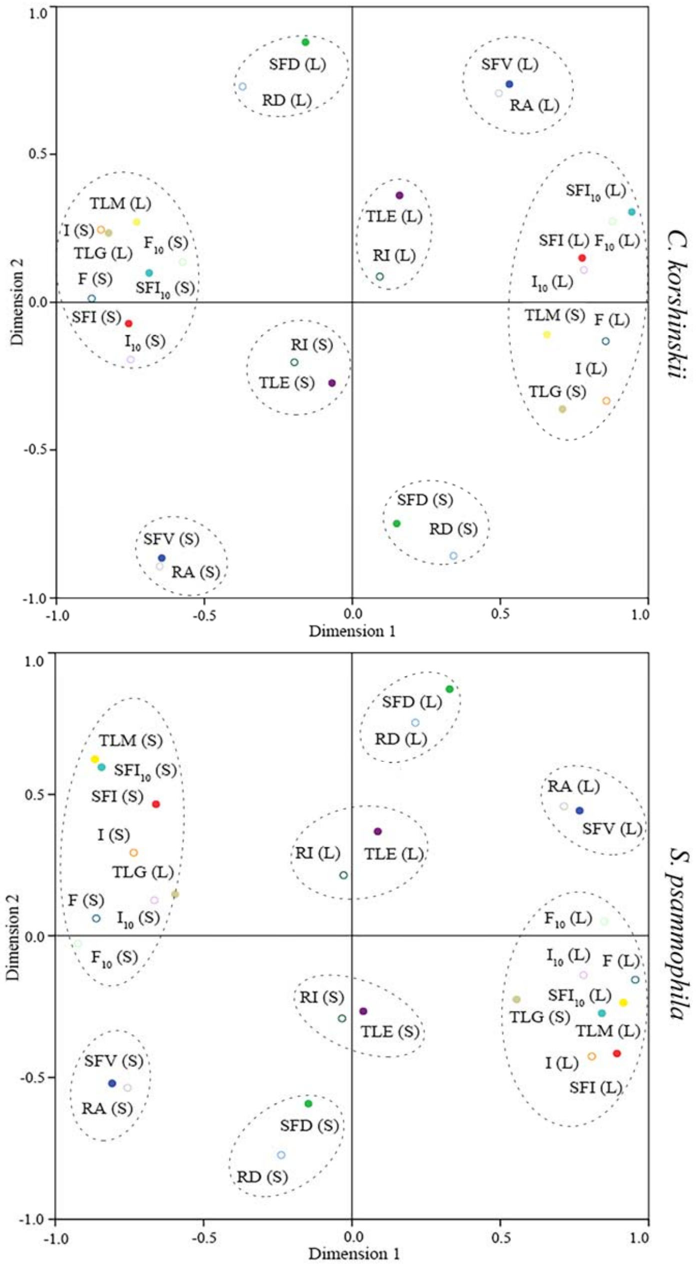

Figure 5. Correspondence map of stemflow variables with rainfall characteristics for *C. korshinskii* and *S. psammophila*.

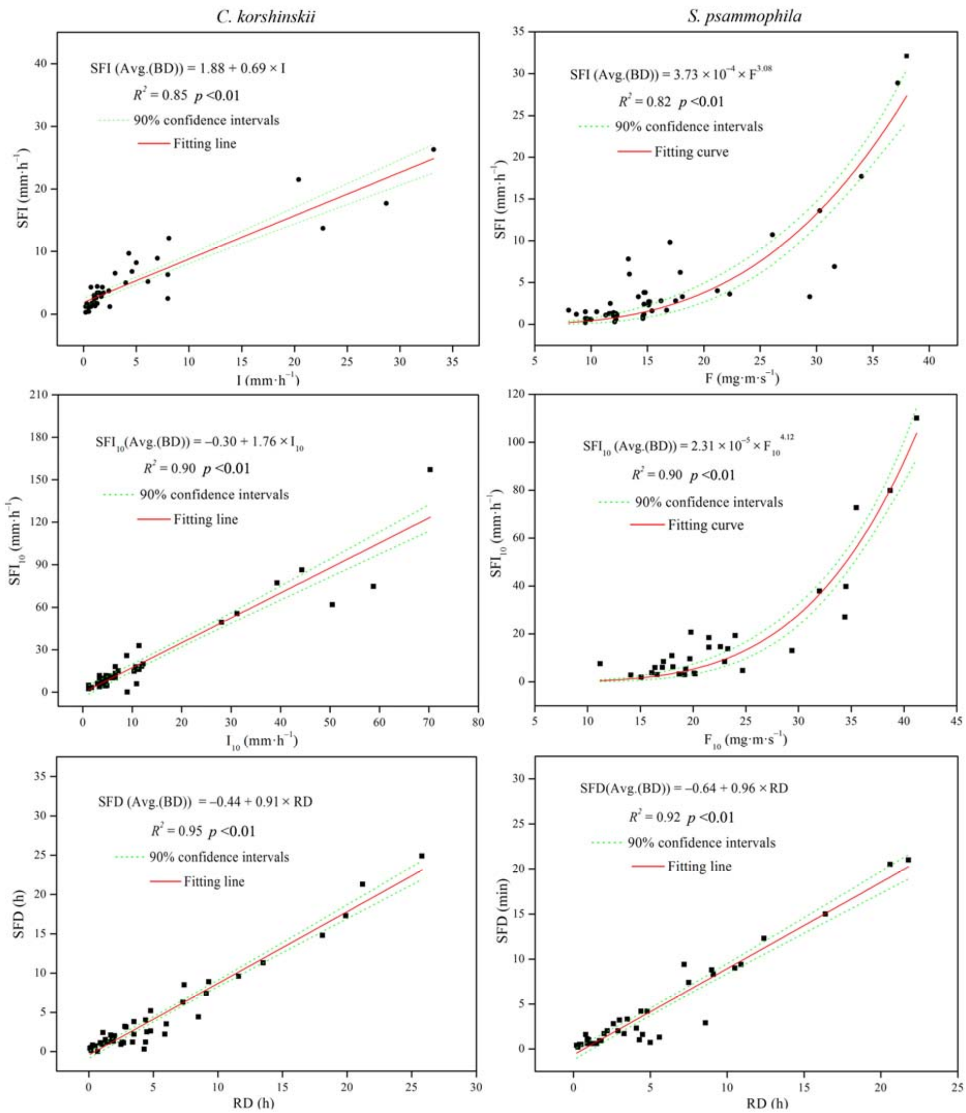

691

692 **Figure 6.** Relationships of stemflow intensity and duration with rainfall characteristics.

https://doi.org/10.5194/hess-2019-254
Preprint. Discussion started: 28 May 2019

Hydrology and Earth System Sciences
Discussions

693 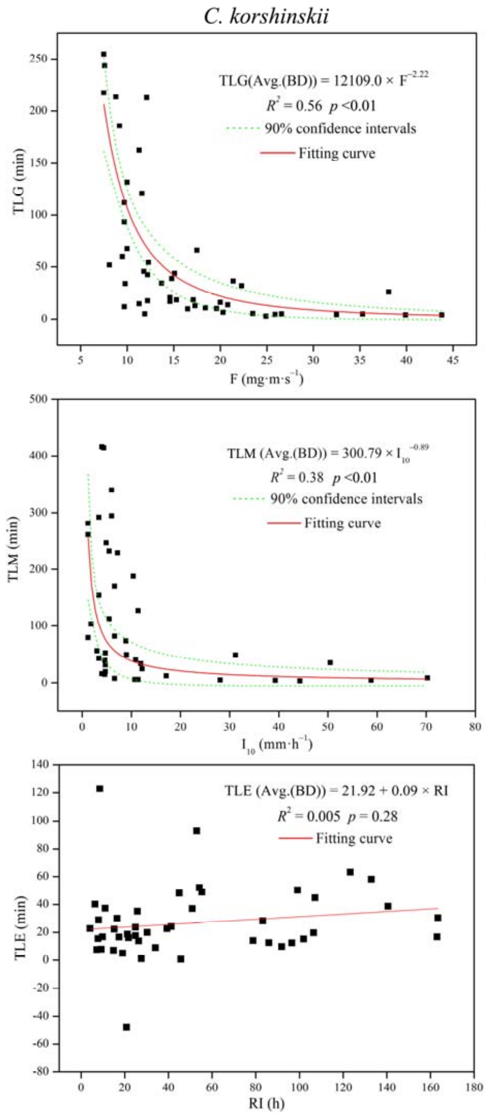

694 **Figure 7.** Relationships of stemflow time lags with rainfall characteristics.